Available online at www.sciencedirect.com

SciVerse ScienceDirect

Ceramics International 38 (2012) 1157–1165

CERAMICS INTERNATIONAL

www.elsevier.com/locate/ceramint

Effect of Nb-doping on dielectric, ferroelectric and conduction behaviour of lead free $Bi_{0.5}(Na_{0.5}K_{0.5})_{0.5}TiO_3$ ceramic

Krishan Kumar, Binay Kumar *

Crystal Lab, Department of Physics & Astrophysics, University of Delhi, Delhi 110007, India

Received 8 July 2011; accepted 19 August 2011
Available online 6 September 2011

Abstract

$Bi_{0.5}(Na_{0.5}K_{0.5})_{0.5}TiO_3 + y$ wt.% Nb ($y = 0$–1) piezoelectric ceramics were synthesized by solid state reaction. The effect of varying Nb concentration on various properties of BNKT ceramic has been investigated in detail. The effect of Nb-doping on dielectric and ferroelectric property has been presented. An increase in its depolarization temperature and Curie temperature with Nb concentration was observed. The electrical properties of pure and Nb-doped BNKT ceramic over a wide range of frequencies (20 Hz to 2 MHz) and temperature (30–430 °C) were studied using impedance spectroscopic technique.

Keywords: A. Sintering; B. Grain boundaries; C. Dielectric Properties; C. Ferroelectirc Properties

1. Introduction

High performance piezoelectric materials find potential applications in sophisticated research, medical and defense devices like piezoelectric sensors, transducers and actuators. To date, PZT is the most widely exploited and extensively used piezoelectric material [1,2]. However, considering the toxicity of lead present in PZT, there is a greater demand for the development of environmental friendly lead-free piezoelectric materials [3–5]. Several lead free materials are now being investigated in search of potentially attractive alternatives to PZT for specific applications.

Bismuth sodium titanate, $Bi_{0.5}Na_{0.5}TiO_3$ (BNT) is a rhombohedral perovskite like structure with Bi^{3+}, Na^+ ions distributed randomly in the A-Site. It exhibits a high transition temperature ($T_c \sim 320$ °C), good ferroelectric properties, a large remanent polarization ($P_r \sim 38$ (C/cm^2) and coercive field ($E_c = 73$ kV/cm) at room temperature [6–9]. In addition, bismuth potassium titanate $Bi_{0.5}K0_{.5}TiO_3$ (BKT) is an excellent lead free piezoelectric ceramic, having a tetragonal symmetry at room temperature and high transition temperature ($T_c = 380$ °C) with a comparatively lower coercive field (~60 kV/cm) [10]. Further, a complex system of BNT and BKT ($Bi_{0.5}(K_xNa_{1-x})_{0.5}TiO_3$) shows a reasonably good piezoelectric property near its morphotropic phase boundary (MPB, $0.16 \leq x \leq 0.2$), as compared to other lead free piezoelectric ceramic [11–14]. Although the material with the composition of $Bi_{0.5}(Na_{0.85}K_{0.15})_{0.5}TiO_3$ has been studied well because this composition lies on the morphotropic phase boundary [15,16]. BNKT50 is selected in this work because of the following reason. The ferroelectric state of co-existence between the rhombohedral phase of BNT and tetragonal phase of BKT at morphotropic phase boundary are not as stable as the single phase of BNT and BKT, respectively. In addition, an optimum poled BNKT50 ceramics are found to show relatively high piezoelectric properties, a high T_d-value and low dielectric loss, which makes it a better composition for working at relatively higher temperature [17]. However, BNKT50 suffers from some problems as mentioned below which need to be addressed before it can be presented as a safer alternative to the lead based PZT ceramic:

(1) The depolarization temperature T_d, of BNKT is still not very high (~230 °C). It is required to increase the T_d-value.
(2) The coercive field (E_c) is still high which causes problem in the polling process. It is required to decrease the E_c of the samples.

BNKT system belongs to perovskite-type oxides with a general formula ABO_3 where A-site is co-occupied by large

* Corresponding author. Fax: +91 011 27667061.
E-mail addresses: bkumar@physics.du.ac.in, b3kumar69@yahoo.co (B. Kumar).

0272-8842/$36.00
doi:10.1016/j.ceramint.2011.08.045

radius cation viz. Bi, Na, K and B-site is occupied by a small radius cation Ti. Many researchers have undertaken work to enhance the dielectric and piezoelectric properties of BNKT by various ionic substitution at A and B-site [18–20]. Various results on different doping in this binary system have been reported. However, T_d did not show any substantial increase [12,21]. The purpose of the present study is to investigate the effect of varying Nb-content on various physical properties of BNKT50 ($x = 0.5$) ceramic. Further investigations were made to obtain an optimum doping to achieve maximum response with increased depolarization and Curie temperature.

1.1. Experimental procedure

Nb doped BNKT ceramic were synthesized by solid state reaction. Powders of Bi_2O_3, K_2CO_3, Na_2CO_3, TiO_2, and Nb_2O_5 (purity > 99.99% Sigma–Aldrich) were used according to the composition of $Bi_{0.5}(Na_{0.5}K_{0.5})_{0.5}$ $TiO_3 + y$ wt.% Nb ($y = 0$, 0.2, 0.4, 0.6, 0.8 and 1.0 wt.%). After mixing for 10 h, the powder was calcined at 850 °C for 4 h. The obtained calcined powders were regrind and mixed with binder (polyvinyl alcohol) and dried at 150 °C. Pallets of 12 mm dia and ~1.5 mm thickness were sintered at 1050 °C for 4 h. The obtained ceramic was finely grinded and subjected to powder XRD in the range 20–70° of 2θ using PW3710 Philips diffractometer (CuK_α radiation). After polishing and electroding (using high grade silver paste), the samples were subjected to various characterizations. The variation of dielectric constant with temperature at different frequency (100 Hz to 2 MHz) was studied from room temperature to 550 °C using an Agilent make (Model E4980A) impedance analyzer. Ceramic pellets were poled by applying a field of 20 kV/cm at 70 °C for 1 h. The Hysteresis loops were traced using a fully computer interfaced P–E loop tracer based on modified sawyer tower circuit.

2. Result and discussion

The PXRD patterns of Pure and Nb-doped BNKT ceramic is shown in Fig. 1. A pure perovskite phase was observed for pure BNKT ceramic. Apart from a slight shift of the peaks (for Nb-doped BNKT ceramic) towards higher angle, no other significant difference in the XRD pattern was observed. The obtained XRD patterns were subjected to cell refinement using X'Pert High Score Plus software and found to have tetragonal symmetry (space group 4 mm) with cell parameters $a = b = 3.837$ Å and $c = 4.132$ Å and $\alpha = \beta = \gamma = 90°$, which is in good agreement with earlier reported value [22].

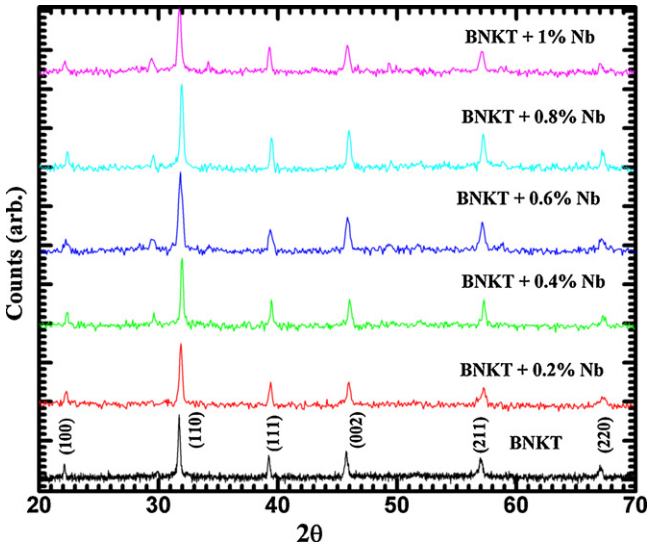

Fig. 1. X-ray diffraction pattern with various doping concentration of pure and Nb-doped BNKT ceramic at room temperature.

Fig. 2 shows the temperature dependence of dielectric constant for pure and Nb-doped BNKT ceramic at 1 kHz. A three fold increase in the value of dielectric constant was observed in the doped samples (Table 1). The value of dielectric constant at room temperature for pure and Nb-doped (0.2%, 0.4%, 0.6%, 0.8% and 1.0%) BNKT ceramics were found to be 371, 1837, 1483, 1247, 1021 and 2961, respectively. In addition, for the present case, a higher value of dielectric constant than that of BNKT synthesized at MPB was observed [23]. This increase in dielectric constant by Nb-addition is due to an increase in the superparaelectric clusters in the ceramic

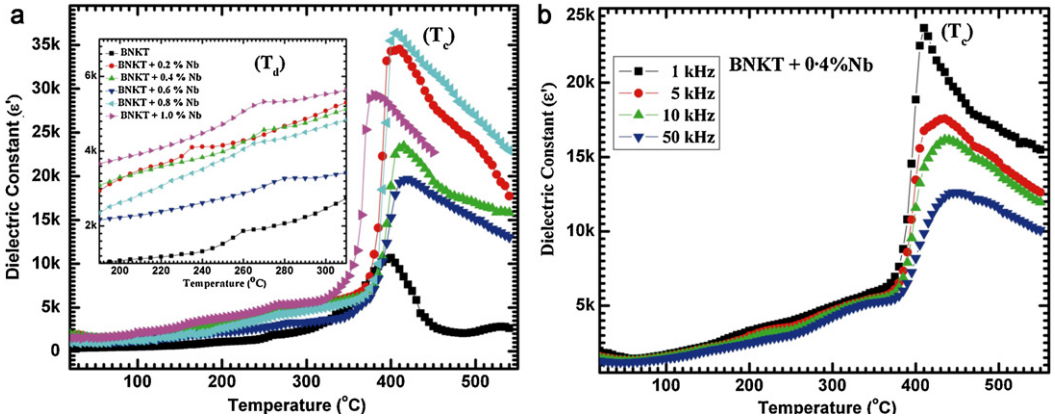

Fig. 2. (a) Variation of dielectric constant with temperature for various doping concentration of Nb at 1 kHz. Inset figure shows the peak corresponding to T_d for all the samples. (b) Variation of dielectric constant for 0.4% Nb-doped BNKT ceramic at different frequencies.

Table 1
The values of T_d, T_m and $\acute{e}$ of pure and Nb-doped BNKT ceramics at different frequencies.

Freq (kHz)	BNKT			BNKT + 0.2% Nb			BNKT + 0.4% Nb			BNKT + 0.6% Nb			BNKT + 0.8% Nb			BNKT + 1.0% Nb		
	T_d (°C)	T_m (°C)	$\acute{e}$ (k)	T_d (°C)	T_m (°C)	$\acute{e}$ (k)	T_d (°C)	T_m (°C)	$\acute{e}$ (k)	T_d (°C)	T_m (°C)	$\acute{e}$ (k)	T_d (°C)	T_m (°C)	$\acute{e}$ (k)	T_d (°C)	T_m (°C)	$\acute{e}$ (k)
1	260	400	10.66	220	410	34.86	270	420	23.67	280	405	19.48	265	400	36.35	270	370	30.45
5	265	405	4.07	230	410	22.30	290	435	17.58	290	415	13.28	270	400	22.90	275	380	20.84
10	265	410	2.96	235	420	18.06	300	440	16.16	305	420	11.00	275	405	18.20	280	385	17.50
50	270	415	1.63	240	435	13.36	300	450	12.61	315	425	7.17	280	410	10.55	285	390	11.67

[24]. The behaviour of the dielectric constant is also strongly dependent on the BKT concentration above the MPB [25]. The variation of dielectric constant with temperature reveled two phase transitions which corresponds to the depolarization phase transition in lower temperature range (230–285 °C, inset, Fig. 2) and Curie phase transition at higher temperature range (380–420 °C). Further, the value of T_c and T_d was found to increase with Nb concentration till 0.4%, beyond which it decreases (Table 1).

A Similar trend for these properties with different doping was observed by many researchers. Jiang et al. have reported the variation of T_c with Mn doping concentration of 0.2, 0.4 and 0.5 wt.% and found that the value of T_c is maximum for the 0.4% Mn-doped BNKT ceramic [23]. Fu et al. have studied the variation of dielectric constant of BNBT ceramic as a function of Nd_2O_3 variation in the range of 0.2%, 0.4%, 0.6% and 0.8% and found that the maximum value of dielectric constant is for 0.4% Nd_2O_3-doped BNBT ceramic [24].

The temperature dependence of dielectric constant showed an increase in the temperature of dielectric maxima with frequency, which confirms the relaxation behaviour of 0.4% Nb-doped BNKT ceramic (Fig. 2b). A similar behaviour was observed for all the samples. This relaxor behaviour can be explained on the basis of compositional fluctuation and/or random local electric fields and stress-induced phase transition due to Na^+ and Bi^+ ions distributed randomly in the A-site [9,10]. Further, the effect of Nb addition will also depends on the site on which Nb^{5+} ions have entered. The Nb ions enter at B-site due to the similar ionic size of Nb^{5+} (0.69 Å) and Ti^{4+} (0.60 Å) [27]. It is well known that for higher sintering temperature, easily volatile ion bismuth is evaporated and oxygen vacancies are created for neutralization. These defects viz. bismuth and oxygen vacancies are considered to be the most mobile charges and play an important role in various electrical parameters of the sample. This oxygen vacancies created during sintering at higher temperature is also accompanied by the Ti valance transition from Ti^{4+} to Ti^{3+} [28]. This transition is due to the placement of an electron in the empty 3d. In addition, the Nb ions that substitute Ti ions at B-site also undergo similar transition from Nb^{5+} or Nb^{3+} to compensate the charge due to oxygen vacancy [29].

Smolenskii et al. in 1970 reported that the dielectric dispersion of relaxor ferroelectric materials deviates strongly from Curie–Weiss law as the temperature T_m was approached from high temperature [26]. They found that Curie–Weiss behaviour is retained for the temperature range far greater than T_m. The temperature, at which the deviation from Curie–Weiss behaviour occurs, is close to the temperature of onset of local polarization, T_B (burn temperature; temperature at which the polarization becomes zero for any relaxor ferroelectric material, far above its Curie point) due to the development of correlations between the dipoles. To explain the low frequency dielectric dispersion in PMN, Smolensky proposed a quadratic law given as

$$\frac{1}{\varepsilon} = \frac{1}{\varepsilon_m} + \frac{(T - T_m)^2}{2\varepsilon_m \delta^2} \quad (1)$$

where ε and ε_m are the dielectric constant and its maxima and δ measure of diffuseness. However, it was found that this quadratic law is not suitable to explain the behaviour of all relaxor compounds. Further, the variable power law was introduced to explain the temperature dependence of dielectric constant and is given as

$$\frac{1}{\varepsilon} = \frac{1}{\varepsilon_m} + \frac{(T - T_m)^\gamma}{C} \quad (2)$$

where γ is the diffuseness exponent whose values varies between 1 and 2 and $C = 2\varepsilon_m\delta^2$ in which δ is diffuseness parameter [30,31]. The values of γ and δ are both materials constants depending on the composition and structure of materials [32]. For $\gamma = 1$, the equation reduces to Curie–Weiss

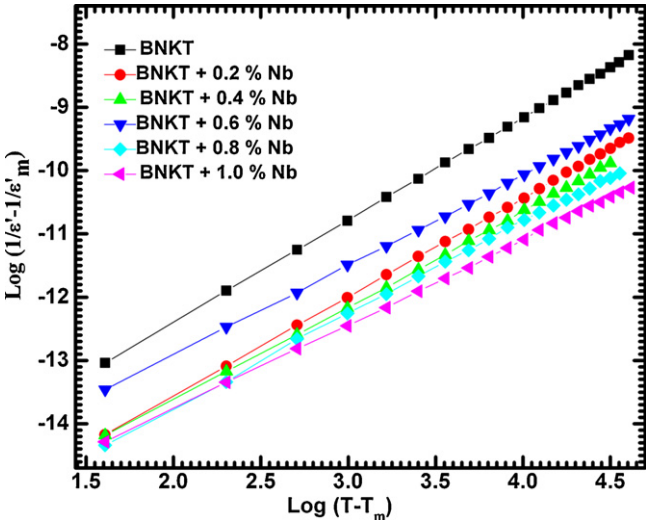

Fig. 3. Plot between $\log(1/\varepsilon - 1/\varepsilon_m)$ versus $\log(T - T_m)$ for all samples at 1 kHz.

Table 2
The values of diffuseness exponent of the phase transition and diffuseness degree of pure and Nb-doped BNKT ceramics at various frequencies.

Frequency (kHz)	BNKT		BNKT + 0.2% Nb		BNKT + 0.4% Nb		BNKT + 0.6% Nb		BNKT + 0.8% Nb		BNKT + 1.0% Nb	
	γ	δ	γ	δ	γ	δ	γ	δ	γ	δ	γ	δ
1	1.58	18	1.56	14	1.34	18	1.50	12	1.64	16	1.20	6
5	1.72	26	1.66	20	1.56	26	1.59	16	1.76	23	1.31	15
10	1.81	29	1.74	24	1.70	31	1.68	20	1.82	28	1.40	19
50	1.91	32	1.89	33	1.93	42	1.86	29	1.90	42	1.47	25

law and for $\gamma = 2$, equivalent to quadratic law proposed by Smolensky. Fig. 3 shows the variation of $\log(1/\varepsilon - 1/\varepsilon_m)$ with $\log(T - T_m)$ for pure and Nb-doped BNKT ceramic at 1 kHz. A similar behaviour was observed for all the frequencies (figures not shown here). The curve is fitted with above equation to calculate the value of γ and δ, which is the expression of the degree of dielectric relaxation and the measure of the degree of diffuseness of the phase transition, respectively. The obtained

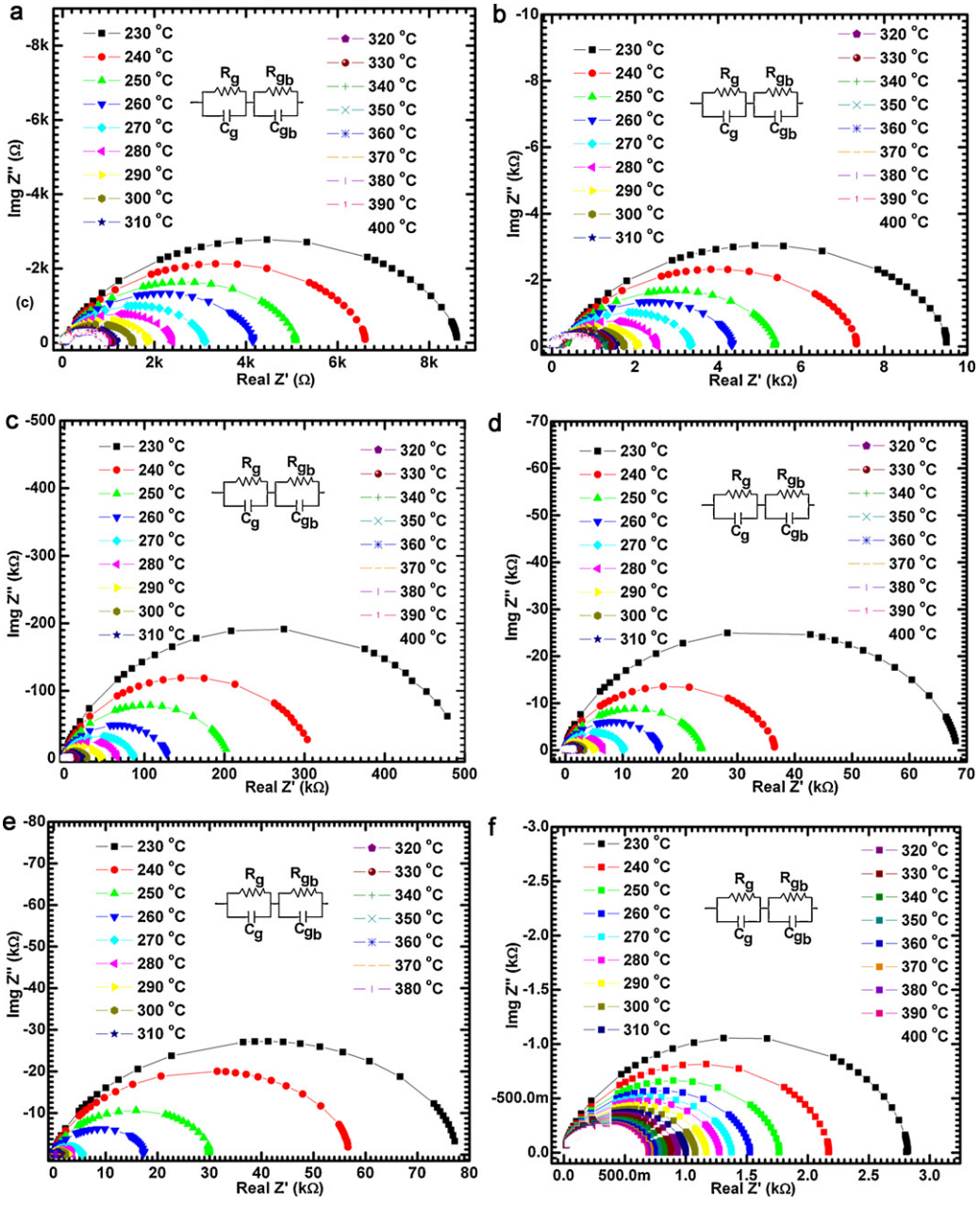

Fig. 4. Nyquist plot of BNKT + y wt.% of Nb (a) $y = 0\%$, (b) $y = 0.2\%$, (c) $y = 0.4\%$, (d) $y = 0.6\%$, (e) $y = 0.8\%$ and (f) $y = 1.0\%$.

values of these parameters for various frequencies are listed in Table 2. The values of γ were calculated by their slope and found to lie in the range 1.49–1.62. The observed diffuse phase transition may be due to the presence of more than one cation in the sub-lattice that produces heterogeneities in the structure and is significant for the relaxation process [33].

The Nyquist plot of pure and Nb-doped BNKT ceramic at different temperatures over a wide frequency range (20 Hz to 2 MHz) are shown in Fig. 4. The impedance data below 200 °C do not take the shape of a semicircle in the Nyquist plot; rather it presents a straight line with large slope, which suggests an insulating behaviour of BNKT ceramic below 200 °C. The slope of the line was found to decrease with increasing temperature in such a way that at 200 °C and beyond it they are found to bend towards Z'-axis and a clear semicircle can be traced out of it. The presence of a depressed semicircle shows the presence of grain (bulk) as well as the grain boundary contribution in all the samples. No other contribution due to electrode was seen in the curve. The decrease in the radius of curvature with increasing temperature shows the increase in the conductivity with temperature for all the samples. This semicircular pattern in the Nyquist plot can be expressed as an equivalent electrical circuit consisting of a parallel combination of two resistive and capacitive (with a constant phase element) elements [21]. The experimental data for all the samples were fitted with an equivalent circuit using Z-View software and is shown in Fig. 4.

A good agreement between the experimental data and the fitted curve was obtained for all the samples. From the obtained value of the combination of resistance and capacitance for grain and grain boundary, respectively, the relaxation time was calculated using the relation $\tau = RC$ and is also listed in Table 3. The relaxation time was found to decrease with increasing temperature for all the samples. The relaxation time is a thermally activated process; hence the variation of these relaxation times was plotted with inverse of temperature and is shown in Fig. 5. The magnitude of the value of τ in the order of 10^{-4} s suggests a hopping conduction mechanism in the system. The obtained plot was fitted with the Arrhenius equation:

$$\tau = \tau_o \exp\left(\frac{-E_{a\tau}}{k_B T}\right) \quad (3)$$

Table 3
Relaxation time and activation energy of conduction for relaxation for various Nb doping using Arrhenius equation.

% Nb	$\tau_o \times 10^{-9}$(G)	E_G (eV)	$\tau_o \times 10^{-9}$(GB)	E_{GB} (eV)
0.0	0.31685	0.46	0.2119	0.45
0.2	0.03483	0.55	0.1419	0.59
0.4	0.01966	0.66	0.0110	0.76
0.6	0.00503	0.67	0.0061	0.78
0.8	0.39482	0.60	0.2919	0.50
1.0	0.02399	0.36	0.0211	0.44

G, grain; GB, grain boundary.

where τ_o is the characteristic relaxation time constant, k_B is the Boltzmann constant and $E_{a\tau}$ is the activation energy for conduction relaxation. The value of $E_{a\tau}$ for all the samples were obtained after fitting the curve and are listed in Table 3. An increase in the value of $E_{a\tau}$ with doping concentration till 0.6% was observed; beyond which it was found to decrease. A similar behaviour was observed in the case of grain boundary as well. In addition, decrease in the activation energy for relaxation for higher doping concentration ($\geq$0.6%) which suggest an increase in the relaxation phenomena in the sample. This may be due the pinning of microscopic dipolar pair because of excess Nb ions in the sample. However, the exact reason for this could not be traced out yet. We are still working on the relaxation behaviour of this system with increased Nb concentration and will be reported in the near future.

2.1. Conductivity analysis

The ac and dc conductivity data were obtained from the impedance data. DC conductivity can be obtained from the Nyquist plot, which ideally resembles a semicircle whose diameter is located on the real x-axis. The dc conductivity is given by

$$\sigma_{dc} = \frac{d}{RA} \quad (4)$$

where d, A and R are the thickness, surface area of the electrode and bulk resistance (calculated from the x-intercept of the impedance Cole–Cole plot). The ac conductivity of the sample

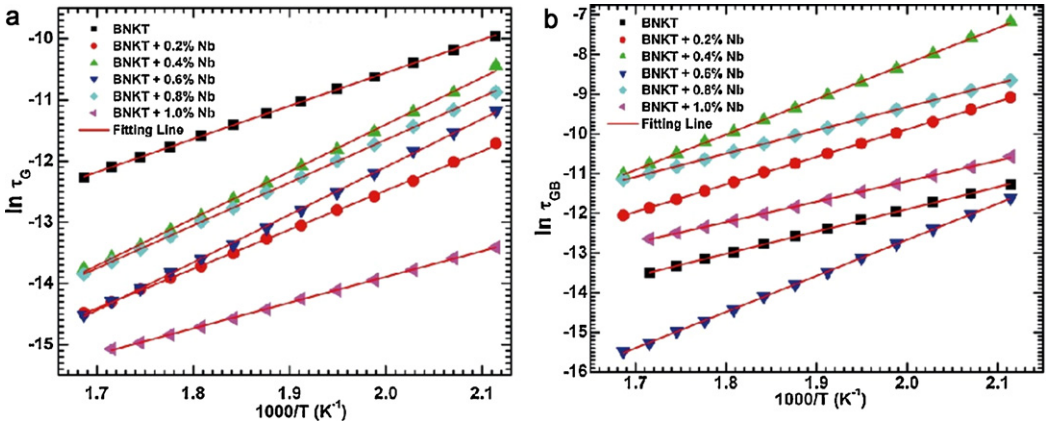

Fig. 5. Relaxation time of (a) grain (b) grain boundary with inverse of temperature.

can be obtained by using the relation

$$\sigma_{ac} = \frac{d}{A}\frac{Z'}{(Z'^2 + Z''^2)} \quad (5)$$

where Z' and Z'' are the real and imaginary parts of impedance.

2.2. Temperature dependence of dc conductivity

The variation of dc conductivity with inverse of temperature is shown in Fig. 6. The dc conductivity for all the samples was found to increase linearly with temperature. However, a slight variation in the value with doping concentration was evident from the curve. The curve was fitted with the Arrhenius equation for conduction given by [34]

$$\sigma = A\exp\left(\frac{-E_a}{k_B T}\right) \quad (6)$$

where E_a is the activation energy, k_B is the Boltzmann's constant and A is pre-exponent factor. The obtained value of activation energy for dc conduction is listed in Table 5. With the doping concentration, the E_a was found to increase till 0.4%, beyond which it decreases. This suggests that the incorporation of Nb ions concentration less than 0.4% restricts the conduction process and hence enhance its usable temperature range. However, incorporation of higher Nb concentration (>0.4%) is found to amplify the conduction process due to the presence of more mobile ions. This increase in the conduction process beyond a specified temperature range usually restricts the usability of any ferroelectric material for real time application. Hence, a moderate doping of Nb will be an added advantage for various applications, where an increase in the conduction process in a specified temperature range is a problem.

In a perovskite system, oxygen vacancies play an important role in conduction process. The activation energy for conduction for oxygen in these systems is nearly 1 eV. Activation energy for the present case was found to be much below 1 eV for most of the samples. These orders of activation energy can also be due to some other relaxing species like mobile dipoles and holes.

The major parameters which affect the conduction behaviour of a system are electrode effect and the defect process. The variation of ac conductivity with frequency at 400 °C is shown in Fig. 7. A similar behaviour was observed at all the temperatures where Nyquist plot can be traced. In the region below 100 kHz, it is apparent that there is a significant contribution from the dc conductivity corresponding to a frequency independent plateau. Further, an increase in the conduction with frequency beyond 100 kHz is due to the existence of microscopic inhomogeneities in the sample and in such case the conduction process can be explained on the basis of hopping conduction [35]. The conduction behaviour with frequency can be formalized to investigate any material using power law given by Jonscher as

$$\sigma_{ac}(\omega) = A\omega^S \quad (7)$$

where A and S are constants at a given temperature. S is a measure of the electrical relaxation behaviour, whose value usually lies in the range of 0–1 [36]. However, to eliminate any contribution of dc conductivity in the sample the modified equation was used which is given as

$$\sigma_{ac}(\omega) = \sigma_{dc} + A\omega^S \quad (8)$$

where σ_{dc} is the dc conductivity [37]. The value of A and S are obtained by fitting the conductivity versus frequency curve at various temperatures by considering the above relation. In present case, the system was found to fit into the above power law, which explains the short range hopping of charges from one site to another, separated by energy barrier of different heights. The obtained values of A and S for different frequencies are listed in Table 4.

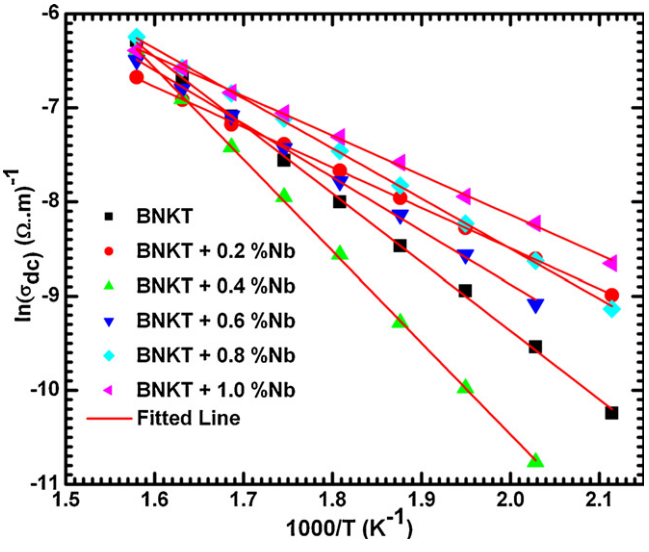

Fig. 6. Variation of dc conduction with inverse of temperature for pure and Nb-doped BNKT ceramic.

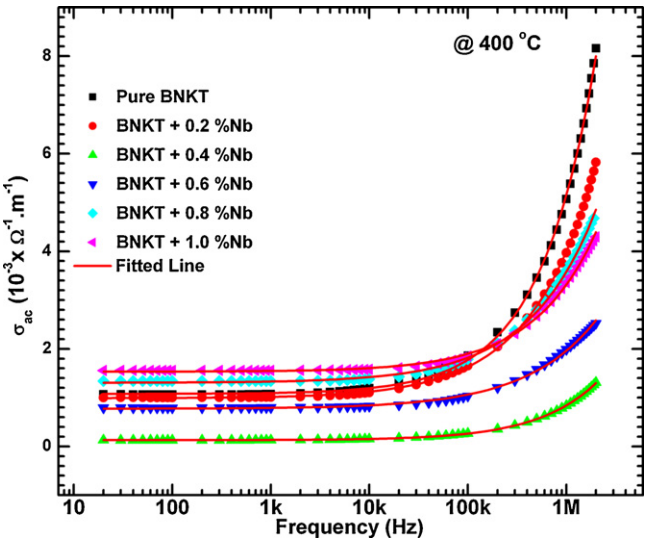

Fig. 7. Variation of ac conductivity with frequency at 400 °C.

Table 4
Fitting parameters for frequency dependence of ac conductivity.

Temp (°C)	Pure		0.2% Nb		0.4% Nb		0.6% Nb		0.8% Nb		1.0% Nb	
	A (10^{-7})	S	A (10^{-6})	S	A (10^{-10})	S	A (10^{-7})	S	A (10^{-7})	S	A (10^{-7})	S
300	2.30	0.71	4.57	0.48	5.91	0.91	0.45	0.73	0.20	0.87	3.71	0.61
320	3.78	0.68	1.35	0.58	0.60	0.85	1.19	0.67	0.33	0.83	2.95	0.63
340	4.68	0.66	0.68	0.63	0.02	0.78	2.54	0.62	4.84	0.61	2.47	0.65
360	0.42	0.85	0.29	0.67	0.03	0.74	3.00	0.60	4.42	0.62	2.01	0.66
380	1.19	0.77	0.25	0.68	0.04	0.72	2.95	0.60	4.08	0.63	1.67	0.67
400	1.03	0.77	0.29	0.67	0.04	0.72	2.54	0.61	3.13	0.64	1.40	0.68

The variation of ac conductivity with inverse of temperature at 1 kHz is shown in Fig. 8. The electrical conductivity in dielectrics are due to the ordered motion of weakly bound charge particles under the influence of external field and the conduction process are always dominated by the type of charge carriers. Various properties like piezoelectricity/ferroelectricity, dielectric along with poling requirement are greatly influenced by the conduction process in the sample. Further, the defects associated material like oxygen vacancy, space charge polarization also contributes to it. Hence, the study of electrical conductivity is very important. The variation of electrical conductivity at higher temperature (dominated by the intrinsic conduction process) is given by Eq. (6). The Arrhenius plot of the ac conductivity was also traced in order to determine the activation energy in the temperature range where ln σ exhibits a linear variation with inverse of temperature (Fig. 8 shows the trend at 1 kHz). The activation energies were calculated by curve fitting (Eq. (6)). The obtained activation energy at 1 kHz is for all the samples are listed in Table 5. The activation energy of all samples is less than 1 eV, which shows the conduction is due to the thermal motion of oxygen or due to the formation of associations between oxygen vacancies and residual cations in the grain boundary [38].

Fig. 9 shows the P–E Hysteresis loops of pure and Nb-doped ceramic at room temperature. The value of remnant polarization (in the order of 36 μC/cm^2) was found to increase with Nb concentration till 0.4%. However its coercive field was also found to increase as compared to pure sample. The ferroelectric properties were strongly influenced by composition and its homogeneity, defects, external field and orientation of domain, which eventually contribute to the material response. Uniform oriented domain structure actually increases the ferroelectric properties. For 0.4% Nb-doped BNKT ceramic, high value of P_r shows the presence of more uniform domain structure [39]. It may be concluded that with the increase of doping concentration beyond 0.4%, the uniformity of the domain structure is disturbed.

According to Haertling and Zimmer, the empirical relation between remnant polarization, saturation polarization and polarization at fields above coercive field is given by the

Table 5
Activation energy for dc and ac conduction with doping concentration.

% Nb	E_{dc} (eV)	E_{ac} (eV) at 1 Hz
0.0	0.63	0.41
0.2	0.37	0.36
0.4	0.84	0.53
0.6	0.50	0.45
0.8	0.46	0.36
1.0	0.36	0.26

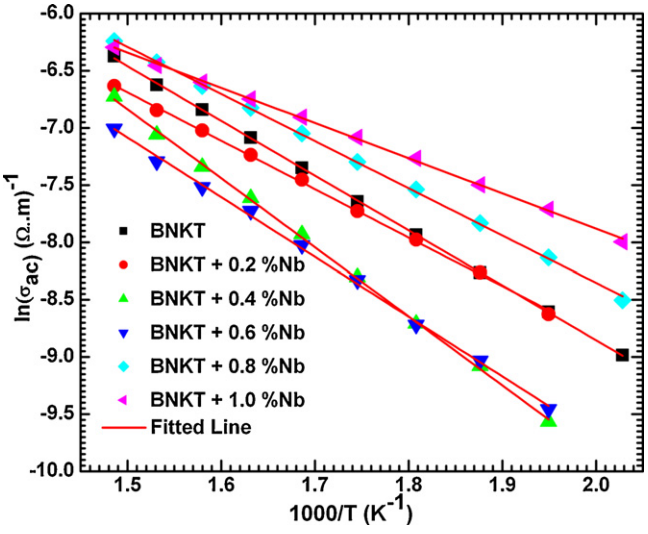

Fig. 8. Variation of ac conductivity with inverse of temperature at 1 kHz.

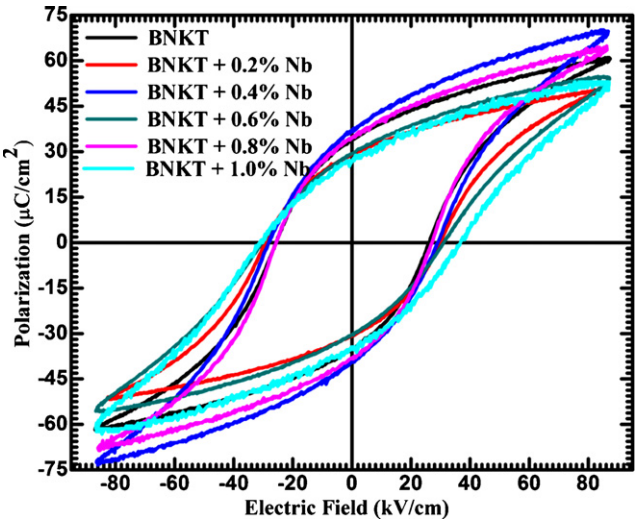

Fig. 9. PE Hysteresis loop for pure and Nb-doped BNKT ceramic.

Table 6
Comparison of various ferroelectric parameters of Pure and Nb-doped BNKT ceramics.

Sample name	P_r (μC/cm^2)	E_c (kV/cm)	R_{sq}
BNKT	33.00	26	1.78
BNKT + 0.2% Nb	29.00	28	1.85
BNKT + 0.4% Nb	36.00	30	1.93
BNKT + 0.6% Nb	30.00	31	1.62
BNKT + 0.8% Nb	35.00	27	1.68
BNKT + 1.0% Nb	27.50	36	1.77

relation [40],

$$R_{sq} = \frac{P_r}{P_s} + \frac{P_{1.1E_c}}{P_r} \quad (9)$$

where R_{sq}, P_s and $P_{1.1E_c}$ are the squareness parameter of Hysteresis loop, saturation polarization and polarization at an electric field equal to 1.1 times the coercive field, respectively. For an ideal Hysteresis loop the squareness parameter is equal to 2. Using this relation, a quantification of changes in the Hysteresis behaviour for each sample can be done. The squareness parameters for all samples were calculated. Further, an increase in R_{sq} for doping samples shows a better switching behaviour of polarization can be achieved with increased Nb concentration. The variation of P_r, E_c and R_{sq} with doping concentration is listed in Table 6.

3. Conclusion

Pure and Nb-doped BNKT ceramics has been synthesized by conventional solid state reaction technique and a pure perovskite phase for all the samples was achieved. The Curie and depolarization temperatures were found to increase with doping concentration till 0.4% of Nb. Further, a higher value of dielectric constant was obtained as a result of doping. All the samples under test were found to exhibit relaxor behaviour with diffuse phase transition. These behaviours were analyzed using various models. A higher degree of relaxation and diffused character was observed for the sample with 0.4% Nb concentration. A single and slightly depressed semicircle in Nyquist plot for all the samples confirmed the effect of bulk as well as grain boundary contribution. The Nyquist plots were fitted for two parallel combinations of R and C. Activation energy for relaxation ($E_{a\tau}$) for BNKT ceramic was found to increase with Nb doping till 0.6%. The order of ($E_{a\tau}$) in the present case suggested the hopping conduction mechanism in the system due to the thermal motion of oxygen. This was further confirmed from the order of activation energy (E_a) observed for dc conduction. In addition, the value of activation energy for ac conduction was found to decrease with increasing frequency. The value of E_a ac conduction also suggested a short range hoping conduction. A higher value of remnant polarization in the case of 0.4% doped sample was observed. On the basis of all experimental observations, 0.4% Nb doping can be considered as an optimum doping to achieve an enhanced and improved performance of BNKT ceramic in a wide temperature and frequency range.

Acknowledgements

We are thankful for the financial support received from the Department of Science & Technology, India, through SERC project ''Growth of device level lead free alkali-based piezoelectric single crystals (SR/S2/CMP-0068/2010)''. K. Kumar is thankful to UGC for research fellowship in 'Science for Meritorious Students'.

References

[1] B. Jaffe, W.R. Cook, H. Jaffe, Piezoelectric Ceramics, Academic Press, London, 1971, pp. 115–181.
[2] T. Yamamoto, Ferroelectric properties of the $PbZrO_3$–$PbTiO_3$ system, Jpn. J. Appl. Phys. 35 (1996) 5104–5108.
[3] P.K. Panda, Review environmental friendly lead-free piezoelectric materials, J. Mater. Sci. 44 (2009) 5049–5062.
[4] E. Cross, Lead-free at last, Nature 4 (2004) 24–25.
[5] Y. Saito, H. Takao, T. Tani, T. Nonoyama, K. Takatori, T. Homma, Lead-free piezoceramics, Nature 432 (2004) 84–87.
[6] X.X. Wang, K.W. Kwok, X.G. Tang, H.L. Chan, C.L. Choy, Electromechanical properties and dielectric behavior of $Bi_{1/2}Na_{1/2(1-1.5x)}Bi_xTiO_3$ lead-free piezoelectric ceramics, Solid State Commun. 129 (2004) 319–323.
[7] D.S. Lee, S.J. Jeong, E.C. Park, J.S. Song, Characteristic of grain oriented $(Bi_{0.5}Na_{0.5})TiO_3$–$BaTiO_3$ ceramics, J. Electroceram. 17 (2006) 505–508.
[8] X. Wang, H.L.W. Chan, C.L. Choy, $(Bi_{1/2}Na_{1/2})TiO_3$–$Ba(Cu_{1/2}W_{1/2})O_3$ lead-free piezoelectric ceramics, J. Am. Ceram. Soc. 86 (2003) 1809–1811.
[9] L. Gao, Y. Huang, Y. HU, H. Du, Dielectric and ferroelectric properties of $(1-x)BaTiO_3$–$xBi_{0.5}Na_{0.5}TiO_3$ ceramics, Ceram. Int. 33 (2007) 1041–1046.
[10] Y. Hiruma, K. Marumo, R. Aoyagi, H. Nagata, T. Takenaka, Ferroelectric and piezoelectric properties of $(Bi_{1/2}K_{1/2})TiO_3$ ceramics fabricated by hot-pressing method, J. Electroceram. 21 (2008) 296–299.
[11] A. Sasaki, T. Chiba, Y. Mamiya, E. Otsuki, Dilectric, Piezoelectric properties of $(Bi_{0.5}Na_{0.5})TiO_3$–$(Bi_{0.5}K_{0.5})TiO_3$ systems, Jpn. J. Appl. Phys. 38 (1999) 5564–5567.
[12] T. Takenaka, H. Nagata, Current status and prospects of lead-free piezoelectric ceramics, J. Eur. Ceram. Soc. 25 (2005) 2693–2700.
[13] W. Zhao, H. Zhou, Y. Yan, Preparation and characterization of textured $Bi_{0.5}(Na_{0.8}K_{0.2})_{0.5}TiO_3$ ceramics by reactive templated grain growth, Mater. Lett. 62 (2008) 1219–1222.
[14] C. Peng, J.F. Li, W. Gong, Preparation and properties of $(Bi_{1/2}Na_{1/2})TiO_3$–$Ba(Ti,Zr)O_3$ lead-free piezoelectric ceramics, Mater. Lett. 59 (2008) 1576–1580.
[15] K. Fuse, T. Kimura, Effect of particle sizes of starting materials on microstructure development in textured $Bi_{0.5}(Na_{0.5}K_{0.5})_{0.5}TiO_3$, J. Am. Ceram. Soc. 89 (2006) 1957–1964.
[16] E. Fukuchi, T. Kimura, T. Tani, T. Takeuchi, Y. Saito, Effect of potassium concentration on the grain orientation in bismuth sodium potassium titanate, J. Am. Ceram. Soc. 85 (2002) 1461–1466.
[17] S. Zhao, G. Li, A. Ding, T. Wang, Q. Yin, Ferroelectric and piezoelectric propertie of $(Na, K)_{0.5}Bi_{0.5}TiO_3$ lead free ceramics, J. Phys. D Appl. Phys. 39 (2006) 2277–2281.
[18] B.K. Krishan Kumar, M.K. Singh, N. Gupta, Sinha, Binay Kumar, Enhancement in dielectric and ferroelectric properties of lead free $Bi_{0.5}(Na_{0.5}K_{0.5})_{0.5}TiO_3$ ceramics by Sb-doping, Ceram. Int. (2011), doi:10.1016/j.ceramint.2011.04.013.
[19] D. Lin, D. Xiao, J. Zhu, P. Yu, Piezoelectric and ferroelectric properties of $[Bi_{0.5}(Na_{1-x-y})K_xLi_y)_{0.5}]TiO_3$ lead-free piezoelectric ceramics, Appl. Phys. Lett. 88 (2006) 62901–62903.

[20] Z. Yang, Y. Hou, B. Liu, L. Wei, Structure and electrical properties of Nd_2O_3-doped $0.82Bi_{0.5}Na_{0.5}TiO_3$–$0.18Bi_{0.5}K_{0.5}TiO_3$ ceramics, Ceram. Int. 35 (2009) 1423–1427.

[21] M. Zhu, H. Hu, N. Lei, Y. Hou, H. Yan, MnO modification on microstructure and electrical properties of lead-free $Bi_{0.485}Na_{0.425}K_{0.06}Ba_{0.03}TiO_3$ solid solution around morphotropic phase boundary, Int. J. Appl. Cearm. Technol. 7 (2010) E107–E1137.

[22] X. Yi, H. Chen, W. Cao, M. Zhao, D. Yang, G. Ma, C. Yang, J. Han, Flux growth and characterization of lead-free piezoelectric single crystal $[Bi_{0.5}(Na_{1-x}K_x)_{0.5}]TiO_3$, J. Cryst. Growth 281 (2005) 365–369.

[23] X.P. Jiang, L.Z. Li, M. Zeng, H.L.W. Chan, Dielectric properties of Mn-doped $(Na_{0.8}K_{0.2})_{0.5}Bi_{0.5}TiO_3$ ceramics, Mater. Lett. 60 (2006) 1786–1790.

[24] P. Fu, R. Chu, W. Li, G. Zang, J. Hao, Piezoelectric, ferroelectric and dielectric properties of Nd_2O_3-doped $(Bi_{0.5}Na_{0.5})_{0.94}Ba_{0.06}TiO_3$ lead-free ceramics, Mater. Sci. Eng. B 167 (2010) 161–166.

[25] C.S. Tu, I.G. Siny, V.H. Schmidt, Sequence of dielectric anomalies and high temperature relaxation behavior in $Na_{1/2}Bi_{1/2}TiO_3$, Phys. Rev. B 49 (1994) 11550–11559.

[26] G.A. Smolenskii, Jpn. J. Phys. Soc. 28 (1970) 26–37.

[27] P.Y. Chen, C.C. Chou, T.Y. Tseng, H. Chen, Second Phase, Defect formation in $Bi_{0.5}Na_{0.5-x}K_xTiO_3$ ceramics, Jpn. J. Appl. Phys. 49 (2010) 061506–061513.

[28] S.E. Park, S.J. Chung, Ferroic phase transition in $(Na_{1/2}Bi_{1/2})$ TiO_3 crystals, J. Am. Ceram. Soc. 79 (1996) 1290–1296.

[29] B.K. Singh, B. Kumar, Evidence of additional phase transitions at lower temperatures in the ux grown $Pb(Zn_{1/3}Nb_{2/3})_{0.91}Ti_{0.09}O_3$ single crystal, Mater. Lett. 63 (2009) 625–628.

[30] A. Halliyal, U. Kumar, R.E. Newnham, L.E. Cross, Am. Ceram. Soc. Bull. 66 (1987) 671–675.

[31] N. Vittayakorn, G. Rujijanagul, X. Tan, M.A. Marquardt, D.P. Cann, The morphotropic phase boundary and dielectric properties of the $xPb(Zr_{1/2}Ti_{1/2})O_3$–$(1-x)Pb(Ni_{1/3}Nb_{2/3})O_3$ perovskite solid solution, J. Appl. Phys. 96 (2004) 5103–5109.

[32] D.P. Almond, A.R. West, R. Grant, Preparation and characterization of textured $Bi_{0.5}(Na_{0.8}K_{0.2})_{0.5}TiO_3$ ceramics by reactive templated grain growth, Solid State Commun. 44 (1982) 1277–1280.

[33] H. Khemakhem, A. Simon, R.V.D. Muhll, J. Ravez, Relaxor or classical ferroelectric behaviour in ceramics with composition $Ba_{1-x}Na_{x}$-$Ti_{1-x}Nb_xO_3$, J. Phys. Condens. Matter 12 (2000) 5951–5959.

[34] S. Lanfredi, J.F. Carvalho, A.C. Hernades, Electric and dielectric properties of $Bi_{12}TiO_{20}$ single crystals, J. Appl. Phys. 88 (2000) 283–287.

[35] J.C. Dyre, The random barrier model for ac conduction in disordered solids, J. Appl. Phys. 64 (1988) 2456–2468.

[36] A.K. Jonscher, The universal dielectric response, Nature 267 (1977) 673–679.

[37] A.K. Jonscher, Hopping losses in polarisable dielectric media, Nature 250 (1974) 191–193.

[38] J.S. Kima, C.W. Ahn, H.J. Lee, I.W. Kim, B.M. Jin, Nb doping effects on ferroelectric and electrical properties of ferroelectric $Bi_{3.25}La_{0.75}$-$Ti_{1-x}Nb_x)_3O_{12}$ ceramics, Ceram. Int. 30 (2004) 1459–1462.

[39] E.R. Leite, A.M. Scotch, A. Khan, T. Li, H.M. Chan, M.P. Harmer, S.F. Liu, S.E. Park, Chemical heterogeneity in PMN–35PT ceramics and effects on dielectric and piezoelectric properties, J. Am. Ceram. Soc. 85 (2002) 3018–3024.

[40] G.H. Haertling, W.J. Zimmer, Am. Ceram. Soc. Bull. 45 (1966) 1084–1087.